



DOI: 10.46793/41DAS2025.159LJ

Original scientific paper

# CFD INVESTIGATION OF TURBULENT WATER FLOW IN A PIPE ELBOW: ASSESSMENT OF CAVITATION RISK

Pavle LJUBOJEVIĆ<sup>1</sup>, Saša STAŠEVIĆ<sup>2</sup>

- 0000-0002-5546-5046, Faculty of Mechanical Engineering, Kraljice Marije 16, Belgrade, Serbia, E-mail: pljubojevic@mas.bg.ac.rs
  - Faculty of Mechanical Engineering, Kraljice Marije 16, Belgrade, Serbia, E-mail: <u>d16-</u> 2024@studenti.mas.bg.ac.rs

Abstract: In this study, turbulent water flow in a DN65 pipe elbow was analysed at high Reynolds numbers using the OpenFOAM software with a two-dimensional model. The research aims to determine the critical mean inlet velocity of the fluid—water that leads to a pressure drop below the saturation pressure and the onset of vapour phase formation, i.e., cavitation. Although such elbows in practice usually operate at lower flow rates, corresponding to fluid velocities that do not reach cavitation conditions, here the limiting conditions were examined for potential non-standard applications involving extremely high flow rates resulting in large velocities. After developing the turbulent flow model, the visualisation was performed in ParaView, and the data were subsequently processed in Python, where the cavitation zone areas were calculated.

**Keywords:** cavitation; turbulent flow; CFD; pipe-elbow flow

#### 1. Introduction

Cavitation represents the formation and subsequent collapse of vapor or gas bubbles in the vicinity of solid surfaces [1, 2]. Depending on the mechanism of initiation, cavitation can be classified as hydrodynamic, acoustic, optical, or particle cavitation. Broadly, these phenomena may be grouped into two categories: cavitation induced by stress in liquids (hydrodynamic and acoustic) and cavitation induced by localised energy deposition (optical and particle) [3].

In mechanical systems, particularly in fluid transport applications, hydrodynamic cavitation is the most common type and is associated with adverse effects such as noise, vibration, and a reduction in the load-carrying capacity and durability of machine elements (gears and bearings) [4, 5]. A combined mechanism, referred to as hydrodynamic-acoustic cavitation (HAC), arises when structural vibrations at specific natural frequencies, or other excitation sources, produce pressure fluctuations that promote bubble formation under the influence of ultrasound. In such cases, acoustic cavitation act synergistically with hydrodynamic cavitation, resulting in more severe material degradation within the system [6]. Both hydrodynamic and acoustic cavitation processes generally progress through four characteristic stages: incubation, acceleration, deceleration, and terminal stage. Potentially, a fifth phase may also appear, which refers to

the complete degradation of the work and the consequences of which can be catastrophic [7].

In fluid transport piping systems, cavitation arises in regions where the local pressure decreases below the saturation pressure. Such conditions may occur along straight pipe sections due to frictional losses, at abrupt changes in flow direction (e.g., elbows), within various fittings, or in pump impellers. In addition, entrained gas molecules within the liquid often act as nucleation sites for vapour—gas bubble formation, thereby promoting the initiation of cavitation [8–10]. Therefore, one of the key parameters when sizing and determining the geometry of pipelines is protection against cavitation.

In this study, computational fluid dynamics (CFD) simulations using OpenFOAM were conducted to investigate water flow through a DN65 pipe elbow at five different average inlet velocities: 5, 10, 15, 20, and 25 m/s. Although such elbows are not typically subjected to these flow rates in practical applications, the primary objective of this research was to identify the threshold average inlet velocity at which the system pressure falls below the saturation pressure.

# 2. Model development and setup

The simulation setup, its workflow, and the post-processing of the obtained results are schematically shown in Fig. 1.







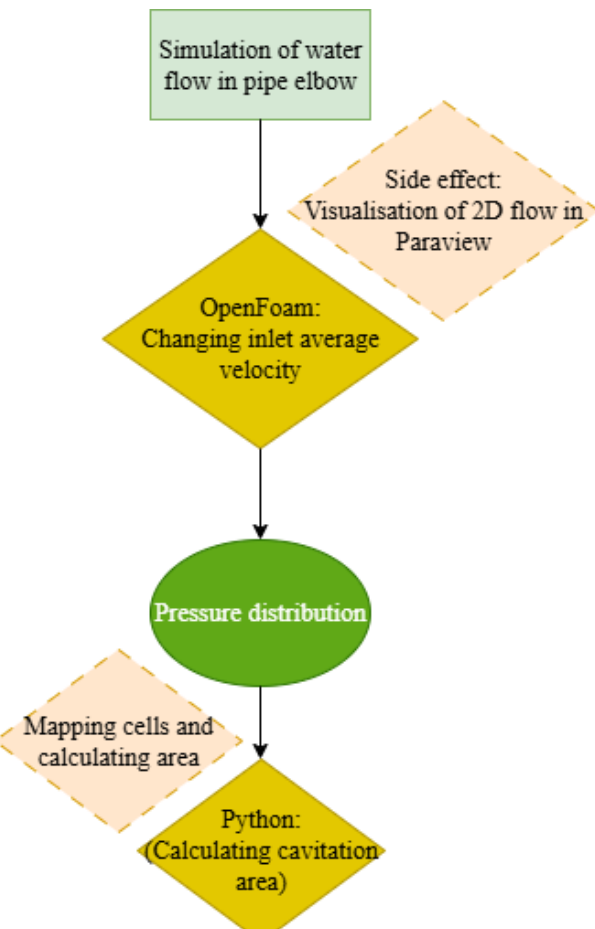


**Fig. 1.** Flow chart of simulation and results processing

The computational domain was defined by the inner pipe diameter (66.1mm), as it represents the fluid region. To reduce computational cost, the pipe was sectioned along the mid-plane, enabling a 2D flow analysis. The pipe geometry and mesh generation were carried out in Gmsh and are illustrated in Fig. 2.

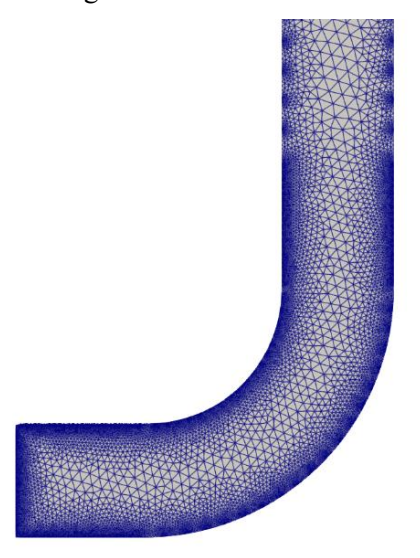


Fig. 2. Pipe elbow model mesh

The mesh consists of a total of 32 884 prismatic cells and one layer in depth to achieve a 2D simulation. The mesh parameters, with a maximum non-orthogonality of 28.82° and an average of 5.87°, indicate excellent mesh accuracy.

The simulation was carried out for water at 20 °C, with the flow considered isothermal. Under these conditions, the kinematic viscosity of water is  $1 \times 10^{-6}$  m<sup>2</sup>/s, and the Reynolds numbers for the inlet velocities are given in Table 1.

Table 1. Reynolds number values

U <sub>avg</sub> [m/s]	5	10	15	20	25
Re/10 <sup>5</sup>	3.3	6.6	9.9	13.2	16.5

These Reynolds number values indicate turbulent flow in the pipe elbow, which is why the RNG k– $\epsilon$  model was selected in the pimpleFoam solver. Since the flow at the inlet to the elbow itself is laminar, in order to avoid extending the pipe upstream of the elbow, following the approach in [11], the inlet velocity profile was prescribed using Equation (1).

$$\frac{\bar{u}}{U_C} = \left(\frac{R-r}{R}\right)^{1/n}, n = f^{-1/2} \tag{1}$$

Where  $U_c$  is velocity in pipe centre, and f is the friction coefficient calculated according following Swamee and Jain modification of Colebrook equation for our values of Reynolds number [12]:

$$f = \left[ -2\log\left(\frac{\varepsilon}{3.7} + \frac{5.74}{Re^{0.9}}\right) \right]^{-2} \tag{2}$$

Where  $\varepsilon$  is relative pipe roughness (0.1mm).

For the validation of the velocity profile, the plot over line option in ParaView was used, and the velocities at the centre were compared with the velocity at the centre obtained according to the following expression (sdhadsh):

$$\frac{U_c}{U_{avg}} = \frac{(n+1)(2n+1)}{2n^2} \tag{3}$$

The plotted velocities at the center and the velocities calculated according to the expression have a relative error of less than 1%.

It is assumed that the fluid is thermally isolated and maintained at a constant temperature of 20  $^{\circ}$ C. The applied model refers to transient flow; however, by comparing the p and U files after a certain number of iterations, very small oscillations of these values were observed, indicating that the flow becomes steady after a certain time. The analysis of pressure distribution was therefore carried out for







these steady-state values. Since the model refers to an incompressible fluid, the pressure values were divided by the water density, meaning that the scales represent pressure per unit mass ( $m^2/s^2$ ). At the outlet of the elbow, the pipe length was set to five diameters due to computational limitations and simulation time. A relative pressure of 200  $m^2/s^2$ , corresponding to an overpressure of 2 bar, was imposed at the outlet. Since this model does not account for fluid compressibility or vapor phase formation, the critical values were taken as pressures in the field corresponding to a scale value of -70, which represents an absolute pressure of  $30 \, \text{kPa}$ , because the saturation pressure of water at  $70 \, ^{\circ}\text{C}$  is  $30 \, \text{kPa}$ .

#### 3. Results and discussion

Fig. 3. shows the velocity field for an average inlet velocity of 20 m/s at three different iterations for visualising the fluid flow.

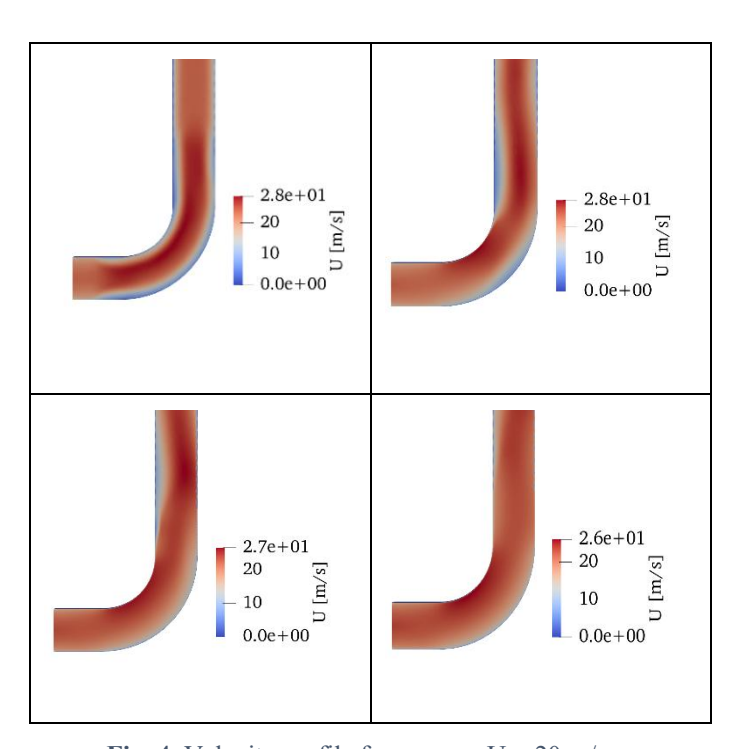


**Fig. 4**. Velocity profile for average U = 20 m/s

The figure shows the initial phase of the flow, followed by the flow development and the velocity profile when it begins to converge, but has not yet reached the steady-state regime.

The analysis of the model was performed for a steady-state flow regime, where the values of the quantities fluctuate negligibly.

The pressure distribution in the model at the final iteration, for the specified simulation duration and

time steps that varied depending on the Courant number, is shown in the figure.

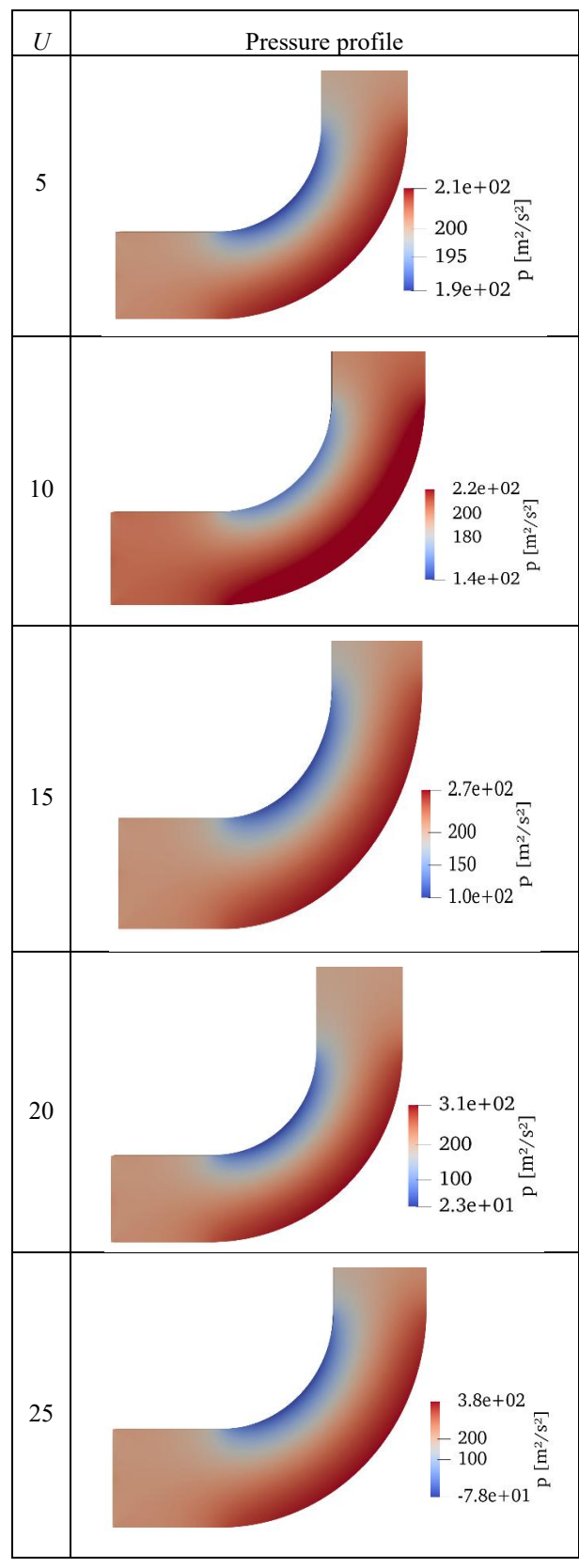


**Fig. 3.** Pressure profile for different average inlet velocities







The pressure scale shows that among the analysed velocities, only 25 m/s leads to a drop of the absolute pressure below the saturation pressure; that is, the critical inlet velocity is slightly below 25 m/s, due to the minimum absolute pressure on the scale being 22 kPa. For an inlet velocity of 20 m/s, the minimum pressure is 23 kPa, above atmospheric pressure, which means that for water at a temperature of 100 °C, a slightly higher velocity than 20 m/s would be critical.

For the final analysis and inspection of the cavitation zone surface, the results from the VTK file were imported into Python, where the cells with pressure below the critical value were mapped and their surface area determined. A total of 21 cells were mapped, with a total surface area of 0.000109 m², which is 0.81% of the total elbow surface area.

#### 4. Conclusions

Based on the brief overview of cavitation in mechanical systems and the conducted simulation, the following conclusions can be drawn:

- Cavitation can represent a major issue in the operation of mechanical systems, primarily in fluid transport systems but also in power transmission systems.
- In pipelines, there is a significant risk of cavitation, which in its final stage can destroy the pipe wall.
- The simulation performed for different inlet velocities shows that the critical average velocity at the inlet of the DN65 elbow for cavitation onset in water at 70 °C is slightly below 25 m/s.
- Since this model does not account for temperature variation, it can also be applied to other water temperatures, but for that reason, it provides a somewhat rougher estimate.
- To validate these results, it is necessary to conduct an experiment and repeat the simulation in a model that supports two-phase flow, in order to possibly track the development of cavitation bubbles.

# Acknowledgments

This work was supported by the Ministry of Science, Technological Development and Innovations of the Republic of Serbia (Contracts: 451-03-137/2025-03/ 200105) and CA23155 - A pan-European network of Ocean Tribology (OTC).

# References

- [1] Knapp, R.T. Cavitation Mechanics and its Relation to the Design of Hydraulic Equipment. Proceedings of the Institution of Mechanical Engineers, 1992 166, 150–163.
- [2] Dojčinović, M. *Razaranje materijala pod dejstvom kavitacije*; Monograph, Tehnološko-metalurški fakultet, Beograd, 2013.
- [3] Lauterborn, W. Cavitation and Inhomogeneities in Underwater Acoustics. In *Proceedings of the First International Conference*, Göttingen, Fed. Rep. of Germany, July 9–11, 1979; Springer Science & Business Media (2012)
- [4] Dowson, D., Taylor, C.M. Cavitation in Bearings. *Annu. Rev. Fluid Mech.*, 1979, 11, 35–65. https://doi.org/10.1146/annurev.fl.11.010179.000 343
- [5] Ouyang, T., Mo, X., Lu, Y., Wang, J. CFD-vibration coupled model for predicting cavitation in gear transmissions. *International Journal of Mechanical Sciences*, 2022, 225.
- [6] Wu, P., Bai, L., Lin, W., Wang, X.: Mechanism and dynamics of hydrodynamic-acoustic cavitation (HAC). *Ultrasonics Sonochemistry*, 2018, 49, 89–96.
- [7] G02 Committee: Test Method for Cavitation Erosion Using Vibratory Apparatus, http://www.astm.org/cgi-bin/resolver.cgi?G32-16
- [8] Chang, H., Xie, X., Zheng, Y., Shu, S., Numerical study on the cavitating flow in liquid hydrogen through elbow pipes with a simplified cavitation model. *International Journal of Hydrogen Energy*, 2017, 42, 18325–18332.
- [9] Jin, Z., Gao, Z., Qian, J., Wu, Z., Sunden, B., A Parametric Study of Hydrodynamic Cavitation Inside Globe Valves. *Journal of Fluids Engineering*, 2018, 140.
- [10] Martin, C.S., Medlarz, H., Wiggert, D.C., Brennen, C., Cavitation Inception in Spool Valves. *Journal of Fluids Engineering*, 1981, 103, 564–575.
- [11] Homicz, G.: Computational Fluid Dynamic simulations of pipe elbow flow, (2004)
- [12] Genic, S., Aranđelović, I., Kolendić, P., Jarić, M., Budimir, N., Genić, V., A Review of Explicit Approximations of Colebrook's Equation. *FME Transaction*, 2011, 39(2), 67-71.